ELSEVIER

Journal of Alloys and Compounds 452 (2008) 73–79

Journal of ALLOYS AND COMPOUNDS

www.elsevier.com/locate/jallcom

Thermodynamic investigation of the Cu–Zr system

Katsunori Yamaguchi [a,*], Young-Cheol Song [b], Toshiaki Yoshida [a], Kimio Itagaki [b]

[a] *Faculty of Engineering, Iwate University, Ueda 4-3-5, Morioka, Iwate 020-8551, Japan*
[b] *Institute of Multidisciplinary Research for Advanced Materials, Tohoku University, Katahira 2-1-1, Aoba-ku, Sendai, Miyagi 980-8577, Japan*

Received 18 September 2006; received in revised form 4 January 2007; accepted 9 January 2007
Available online 22 February 2007

Abstract

High temperature heat contents of the Cu–Zr system alloys were measured over temperature range from 880 to 1470 K using a drop calorimeter. The enthalpies of fusion of some solid compounds were determined by the heat content—temperature plots and the entropies of fusion were calculated. Enthalpies of mixing in the liquid Cu–Zr system were measured by high temperature reaction calorimetry in the concentration range of $x_{Zr} = 0.182$–0.667 at 1443 K. This system has negative enthalpies of mixing over the measured concentration range. The standard enthalpies of formation at 298.15 K of Cu_9Zr_2, $Cu_{51}Zr_{14}$, Cu_8Zr_3, $Cu_{10}Zr_7$ and $CuZr_2$ compounds were determined from the obtained data for the heat contents and enthalpies of mixing. Based on the experimental data, published thermodynamic and phase diagram data, the Cu–Zr binary system was analyzed using Redlich–Kister polynomial equation. The thermodynamic properties and the phase diagram calculated from the optimized parameters agree well with the experimental data.

Keywords: Heat content; Enthalpy; Phase diagram; Calorimeter; Thermodynamic property

1. Introduction

The treatment of zirconium base alloy wastes such as cladding hulls is becoming a serious problem for the sustainable operation of nuclear reprocessing plants. Although melting down is considered to be one of the effective methods to decrease the volume of these wastes or to eliminate some radioactive elements, this process is energy intensive and needs considerably expensive equipments due to the refractory property of the alloys. The authors have noticed that according to the phase diagram of the Cu–Zr binary system [1] molten copper will dissolve a considerable amount of zirconium even at medium temperatures around 1500 K and proposed some processes [2] for treating the zirconium base alloy wastes by using molten copper. The phase diagram and thermodynamic properties such as activities, enthalpies of mixing, enthalpies of formation and heat contents of this system are useful to look for optimum conditions in the proposed processes. On the other hand, over a wide concentration range liquid Cu–Zr alloys have the ability to form an amorphous by rapid quenching [3]. A knowledge of the thermodynamic and kinetic properties of the Cu–Zr alloys are of interest in the information for glass forming tendency. Nevertheless, only few data are reported on the thermodynamic properties of the Cu–Zr binary alloys. The enthalpies of mixing of liquid Cu–Zr alloys have been measured by calorimetry [4–6]. The activities of copper in liquid Cu–Zr alloys have been determined from Kundsen effusion method and mass spectrometry [5,6]. Although enthalpies of formation for the compounds in the Cu–Zr binary system have been reported by high temperature calorimetry, there still remains considerable disagreement between the reported values [4,5,8].

In this study, high temperature heat contents of Cu–Zr alloys were measured over a temperature range from 880 to 1470 K by drop calorimetry. The phase diagram of the Cu–Zr binary system was also determined from the heat contents data, DTA measurements and the metallographic observation of the solidified alloy samples. Enthalpies of mixing in the liquid Cu–Zr system were measured by high temperature reaction calorimetry at 1443 K.

* Corresponding author. Tel.: +81 196 621 6367; fax: +81 196 621 6367.
E-mail address: benko@iwate-u.ac.jp (K. Yamaguchi).

0925-8388/$ – see front matter © 2007 Elsevier B.V. All rights reserved.
doi:10.1016/j.jallcom.2007.01.173

The thermodynamic and phase diagram data obtained in this study together with data from the literature were assessed using a Redlich–Kister polynomial equation [9].

2. Experimental procedures

2.1. Heat content

A drop calorimeter was used to determine the heat content of the alloys. The experimental details of the apparatus have been given in a separate paper [10]. The starting intermetallic compounds were prepared from copper chips (99.99 mass%) and zirconium rods (99.8 mass%). They were melted in ZrO_2 crucibles which were vacuum-sealed in a silica container. They were used as a master alloy for the sample preparation in the experiment. For each experimental run, a total of about 5.5 g of the master alloy and pure copper or zirconium, used to adjust the composition was kept in a ZrO_2 crucible with an inner diameter of 14 mm and height of 10 mm, which was vacuum-sealed in a silica ampoule with a weight of 2.5 g. This assembly was held at a specific temperature T (K). After thermal equilibrium had been reached, the assembly was dropped into the calorimeter. The calorimeter then measured the total heat content of the sample at temperature of T relative to the final equilibrium temperature in the calorimeter, which was held at about 298 K. The experiments were conducted for seven samples having different mole fractions of zirconium, in the temperature range from 880 to 1470 K.

2.2. DTA and metallographic observation

Differential thermal analysis (DTA) measurements and the metallographic observation for the solidified alloy samples were carried out to determine the phase diagram of the Cu–Zr binary system. DTA experiments were conducted with 0.1–0.3 g samples, heated with a rate of 10 K min^{-1} up to 1573 K under argon atmosphere. A sample holder of α-Al_2O_3 with an inner diameter of 4 mm and a height of 5 mm was used for DTA measurement. Inflection temperatures were determined using the derivative of the DTA curves.

The phase relations and liquidus points saturated with solid zirconium were determined from quenched samples. Samples of the required initial composition were held in ZrO_2 crucibles which were vacuum-sealed in silica containers and were heated at the desired temperature for a period of 24 h in order to attain the equilibration. Then, they were taken out of the furnace and quenched in water. The quenched samples were mounted on epoxy resins and polished for electron probe micro analysis (EPMA). Optical microscopy was employed to identify the phases present in the sample. The compositions of liquid and primary solid phases in the samples were analyzed by EPMA.

2.3. Enthalpy of mixing

A Calvet-type twin calorimeter especially constructed for operation at temperature above 1300 K was used to determine the enthalpies of mixing. The details of the calorimeter were described in a previous paper [11]. The construction of the calorimeter designed in the present work is schematically shown in Fig. 1. It consisted of a heating furnace and a calorimeter assembly placed in a silica tube with an inner diameter of 42 mm and a length of 360 mm. The furnace had a heating element made of silicon carbide (SiC) and was connected to a PID controller with a Pt–Pt13Rh thermocouple. The temperature zone was uniform with in a length of 40 mm within ±2 K in a temperature range of 800–1500 K. The calorimeter tube and the details of the construction of the thermopile are shown schematically in Fig. 2. The calorimeter consisted of an alumina tube with an outer diameter of 20 mm, a height of 50 mm and a thickness of 2 mm. The outside surface of the tube was ground with 44 shallow vertical grooves to allow the placement of a 22 couple thermopile. The 22 thermocouple junctions were distributed over the sample section of the calorimeter located at three different levels at about 5 mm distance. The other 22 junctions were placed at the same level forming the reference section. The thermocouples were made from 0.2 mm diameter Pt–Pt13%Rh wire. The thermopile measured the temperature differences between the sample and the reference sections, and the output is fed into a personal computer through a digital voltmeter. Two alumina crucibles with an outer diameter of 15 mm, a thickness of 2 mm and heights of 20 or 5 mm were placed in the sample and the reference sections of the calorimeter, respectively.

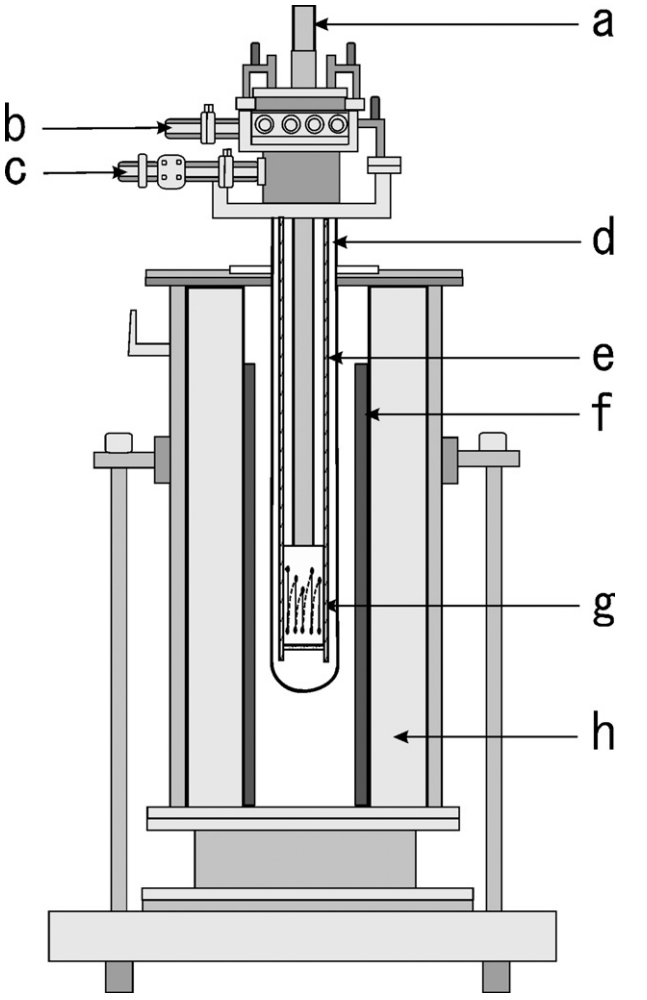

Fig. 1. Construction of high temperature calorimeter: (a) silica drop tube, (b) gas inlet, (c) gas outlet, (d) silica tube, (e) alumina tube, (f) silicon carbide heater, (g) calorimeter section, and (h) insulating material.

The determination of the enthalpies of mixing was performed by the drop method. A typical sample assembly consisted of a ZrO_2 crucible with an inner diameter of 8 mm, a height of 20 mm and a weight of 2 g, which was vacuum-sealed in a quartz cell with an outer diameter of 8 mm, a height of 25 mm, a thickness of 1 mm and a weight of 1.6 g to avoid oxidation of the sample. The cell was supported by a platinum sample holder with an outer diameter of 10 mm, a height of 30 mm and a weight of 3.5 g. Pieces of copper and zirconium of 1.8–2 g were vacuum-sealed in the sample cell. The sample holder was dropped from room temperature into the calorimeter held at 1443 K through a central silica tube. The calorimetric calibration was performed by measuring the thermal effects on dropping the empty container and on dropping the same container in which a reference substance of α-alumina was loaded, the enthalpy value of which was taken from Knacke et al. [12]. The copper metal was supplied in the form of a wire of grade with 99.99 mass% purity. The zirconium metal was a rod with 99.8 mass% purity.

3. Thermodynamic optimization

The experimental phase diagram and thermodynamic properties obtained in the present work together with the values reported in Refs. [4–8] have been assessed thermodynamically. The optimization module integrated in ChemSage (GTT Tech-

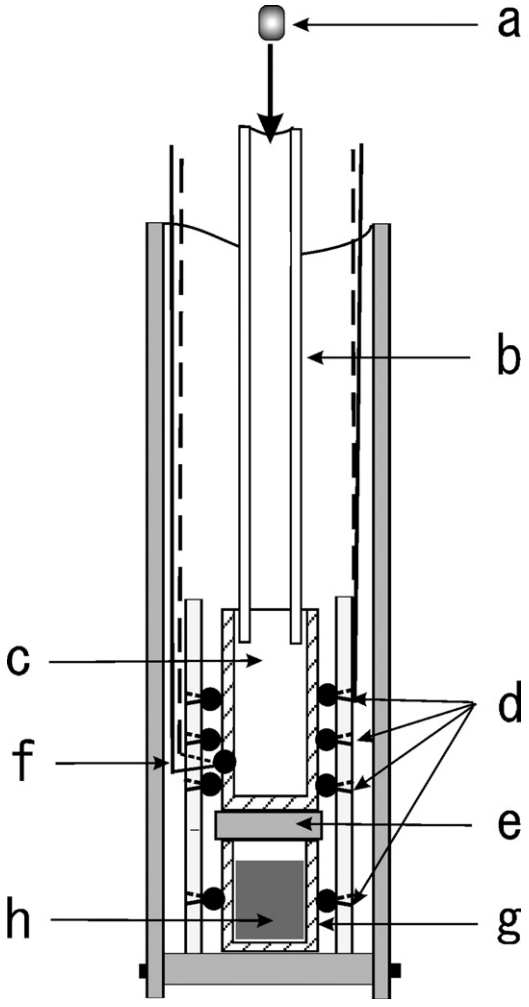

Fig. 2. Schematic diagram of calorimeter cell assembly: (a) sample, (b) silica drop tube, (c) alumina laboratory crucible, (d) thermopile, (e) alumina ring, (f) measuring thermocouple, (g) alumina reference crucible, and (h) alumina block.

nologies, Aachen, Germany) was used for this task [13]. A set of G (Gibbs energy) coefficients for the intermetallic compound phases and ΔG^{E} (the excess Gibbs energy of mixing) coefficients for the liquid phase of the Cu–Zr system were determined by this program. ΔG^{E} is represented by a Redlich–Kister polynomial equation of the form [9]:

$$\Delta G^{E} = x_{Cu}x_{Zr}\Sigma(x_{Cu} - x_{Zr})^{\nu}L^{(\nu)}_{CuZr}(T) \quad (1)$$

where x_{Cu} and x_{Zr} stand for the mole fractions, and the values of $L^{(\nu)}_{CuZr}(T)$ are determined by $L^{(\nu)}_{CuZr}(T) = A^{(\nu)}_{CuZr} - B^{(\nu)}_{CuZr}(T)$. For the pure components of Cu and Zr, and for the intermetallic compounds, a conventional Gibbs energy function of the form:

$$G^{\circ} = a + bT + cT\ln T + dT^2 + eT^3 + \frac{f}{T} + gT^4 + hT^7 + iT^{-9} \quad (2)$$

was used to represent the data of the stable phases.

Table 1
Heat content, $J_T = H_T - H_{298}$, of the Cu–Zr alloys

$x_{Zr}=0.04$		$x_{Zr}=0.081$		$x_{Zr}=0.181$		$x_{Zr}=0.215$		$x_{Zr}=0.273$		$x_{Zr}=0.412$		$x_{Zr}=0.667$	
T (K)	J_T (kJ mol^{-1})	T (K)	J_T (kJ mol^{-1})	T (K)	J_T (kJ mol^{-1})	T (K)	J_T (kJ mol^{-1})	T (K)	J_T (kJ mol^{-1})	T (K)	J_T (kJ mol^{-1})	T (K)	J_T (kJ mol^{-1})
972	23.39	969	26.18	975	24.75	975	23.33	973	18.53	878	18.50	973	21.00
1022	25.59	1021	28.44	1021	26.68	999	23.76	1021	20.02	933	20.55	1022	24.10
1073	27.02	1070	29.71	1071	28.63	1024	24.83	1070	22.00	974	21.16	1075	25.83
1126	28.06	1126	31.81	1122	30.77	1075	28.17	1124	23.59	1021	22.68	1124	28.62
1159	30.27	1146	31.94	1175	32.70	1123	30.20	1171	24.59	1073	23.96	1170	30.76
1191	30.65	1176	33.20	1227	34.01	1173	21.18	1190	26.61	1121	25.52	1196	32.74
1217	32.53	1204	34.20	1251	37.04	1228	34.66	1222	29.65	1146	25.72	1224	35.60
1239	33.89	1226	36.05	1275	41.52	1278	38.25	1253	30.70	1158	28.43	1252	36.30
1251	34.62	1238	37.27	1297	43.31	1326	38.53	1283	32.00	1173	28.48	1261	37.65
1271	41.56	1249	38.44	1323	43.96	1346	41.29	1310	34.67	1183	40.53	1275	37.10
1287	42.53	1260	39.94	1347	45.55	1369	43.43	1341	34.97	1190	13.38	1287	48.05
1302	43.83	1271	40.14	1361	50.18	1380	50.06	1360	37.74	1197	44.33	1299	48.14
1317	49.00	1274	53.49	1372	59.89	1384	51.11	1371	47.46	1223	47.73	1388	51.05
1342	54.91	1283	54.15	1377	60.25	1390	54.46	1383	18.48	1248	47.84	1371	51.18
1368	56.12	1309	55.17	1398	60.84	1394	54.93	1403	50.27	1279	49.50	1406	51.83
1411	57.75	1339	57.05	1426	61.15	1400	61.29	1420	51.55	1294	50.75		
1435	59.27	1371	58.85	1446	61.84	1415	61.80	1453	52.42	1324	51.88		
		1401	60.39			1446	61.80			1342	52.35		
						1468	61.98						

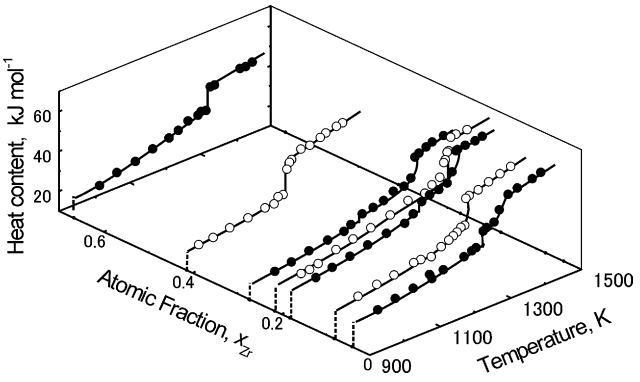

Fig. 3. Heat contents of the Cu–Zr system.

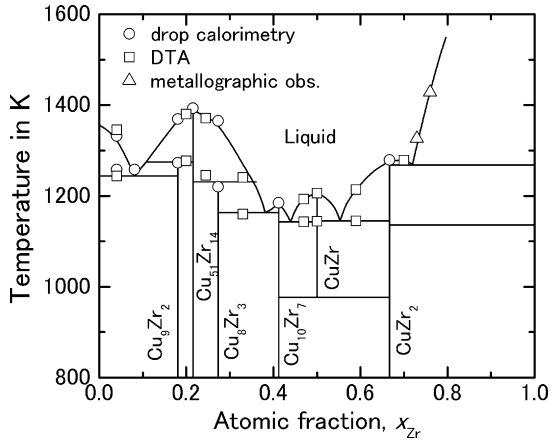

Fig. 4. Experimentally determined phase diagram of the Cu–Zr system: (◯) drop calorimetry, (□) DTA, and (△) metallographic observation.

Table 2
Enthalpy and entropy of fusion of the intermetallic compounds in the Cu–Zr system

Compound	T_m (K)	ΔH_m (kJ mol^{-1})	ΔS_m (J mol^{-1} K^{-1})
$Cu_{51}Zr_{14}$	1393 ± 6	17.85	12.82
$Cu_{10}Zr_7$	1185 ± 3	14.95	12.61
$CuZr_2$	1279	10.95	8.6

4. Results and discussion

The heat contents, $J_T = H_T - H_{298}$, are listed in Table 1 and shown in Fig. 3 in relation to the mole fraction of zirconium. The deflection points in the $J_T - T$ curves correspond to the temperatures of phase changes as well as the solidus and liquidus temperatures. The enthalpies of fusion of some congruent compounds, which were determined by interpolating or extrapolating the heat content values, are summarized in Table 2, along with the calculated entropies of fusion.

The phase transition temperatures determined by DTA experiments or metallographic observations are shown in Table 3. Within the limit of experimental accuracy, the eutectic and peritectic temperatures of less than $x_{Zr} = 0.33$ agree well with literature values [1]. The eutectic temperatures at the composition of $x_{Zr} = 0.47$ and 0.59 are about 20 and 60 K lower than the literature data [1], respectively. The liquidus points of the alloys saturated with solid Zr are in good agreement with the literature phase diagram [1]. On the basis of Fig. 3 and some complementary data, which were obtained in the present study by DTA or the metallographic observation of the solidified samples, the phase diagram of the Cu–Zr system was constructed (Fig. 4).

Table 3
Phase transition temperatures determined by DTA experiments and metallographic observation

x_{Zr}	Temperature (K)			
	Eutectic	Peritectic	Liquidus	Experimental method
0.04	1244	–	1345	DTA
0.20	–	1277	1380	DTA
0.245	–	1245	1371	DTA
0.33	1160	1240	–	DTA
0.47	1143	–	1193	DTA
0.50	1144	–	1206	DTA
0.59	1145	–	1214	DTA
0.70	–	–	1278	DTA
0.73	–	–	1326	Metallographic
0.76	–	–	1428	Metallographic

The enthalpies of mixing of the Cu–Zr alloys were measured for $x_{Zr} = 0.182$, 0.215, 0.273, 0.412 and 0.667 at 1443 K. Enthalpies of dissolution of solid Zr in liquid Cu are summarized in Table 4 and are shown in Fig. 5. In Fig. 6 $\Delta_{dis}H_{s-l}/x_{Zr}$ is plotted against x_{Zr}. These values indicate a linear dependence on the composition. The value extrapolated to pure zirconium composition yields an enthalpy of fusion of zirconium of 20.6 kJ mol^{-1} at 1443 K. This value agrees well with the literature value of 19.3 kJ mol^{-1} estimated from the heat capacities in the solid and the liquid range and the enthalpy of fusion of the pure metal at the melting point 2125 K (18.7 kJ mol^{-1} [12]). The liquid–liquid enthalpies of mixing of the Cu–Zr alloys at 1443 K, $\Delta_{mix}H$, were derived on the basis of the enthalpy of fusion for the pure zirconium and at given in Fig. 7 together with literature results [4–6]. $\Delta_{mix}H$ turned out to be strongly

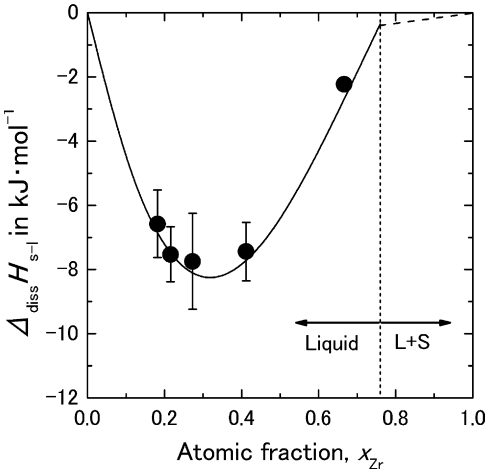

Fig. 5. Enthalpies of dissolution of solid Zr in liquid Cu at 1443 K.

Table 4
Enthalpies of dissolution for the Cu–Zr alloys at 1443 K

x_{Zr}	Cu (g)	Zr (g)	Total (g)	Total (mol)	$\Delta_{diss}H_{s-l}$ (J)	$\Delta_{diss}H_{s-l}$ (kJ mol^{-1})
0.182	1.3648	0.4354	1.8002	0.0263	−175.0	−6.66
0.215	1.1477	0.4523	1.6001	0.0230	−172.3	−7.48
0.273	1.1700	0.6299	1.7999	0.0253	−196.1	−7.75
0.412	0.8977	0.9021	1.7997	0.0240	−178.7	−7.45
0.667	3.8742	11.1252	14.9994	0.1829	−408.4	−2.23

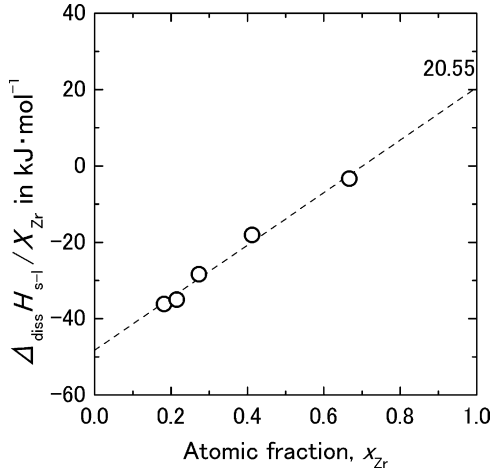

Fig. 6. Plot $\Delta_{diss}H_{s-l}/x_{Zr}$ of against x_{Zr} for the liquid Cu–Zr alloys at 1443 K.

negative. Within the limit of the experimental accuracy and temperature dependence it agrees fairly well with previous data [4–8].

From the solid–liquid enthalpies of dissolution at 1443 K and the heat contents of the compounds determined in this study, the standard enthalpies of formation of the compounds, $\Delta_f H^\circ_{298.15}$, were derived using the following equation:

$$\begin{aligned}&\Delta_f H^\circ_{298.15\,\langle Cu_mZr_n\rangle}\\ &= (m+n)\left\{\Delta_{diss}H_{s-l,1443} - (H_{1443}-H_{298})_{\langle Cu_mZr_n\rangle}\right.\\ &\quad +(1-x_{Zr})\left[\int_{298}^{1358} C_{P,Cu(S)} + \Delta H_{m,Cu} + \int_{1358}^{1443} C_{P,Cu(l)}\right]\\ &\quad \left.+x_{Zr}\int_{298}^{1443} C_{P,Zr}\right\} \qquad (3)\end{aligned}$$

Table 5
Standard enthalpy formation of the Cu_xZr_y compound at 298.15 K

Compound	$\Delta_f H^\circ_{298.15}$(kJ g atom^{-1})			
	Sommer et al. [5]	Kleppa et al. [4]	Ansara et al. [8]	This study
Cu_9Zr_2	−8.7	–	–	−23.8
$Cu_{51}Zr_{14}$	–	−14.07	–	−25.2
Cu_8Zr_3	–	–	–	−16.2
$Cu_{10}Zr_7$	–	−12.3	–	−22.9
$CuZr_2$	–	−11.0	−17.3	−16.6

Table 6
Gibbs energy of the pure components Cu and Zr, and for the intermetallic compounds

Element	G° (J)									Temperature range (K)
	a	b	c	d ($\times10^{-3}$)	e ($\times10^{6}$)	f ($\times10^{-5}$)	g ($\times10^{11}$)	h ($\times10^{21}$)	I ($\times10^{-30}$)	
Cu	−7770.5	130.485	−24.11	−2.657	0.129	0.525	0	0	0	298–1358
Cu	−13542.0	183.804	−31.38	0	0	0	0	0	0.364	1358–3200
Cu (liquid)	5194.3	120.973	−24.11	−2.657	0.129	0.525	0	−5.849	0	298–1358
Cu (liquid)	−46.5	173.881	−31.38	0	0	0	0	0	0	1358–3200
Zr (HCP)	−7827.6	125.649	−24.16	−4.378	0	0.350	0	0	0	298–2128
Zr (HCP)	−26085.9	262.724	−42.14	0	0	0	0	0	−13.429	2128–4000
Zr (BCC)	−525.5	124.946	−25.607	−0.340	−0.010	0.252	−7.614	0	0	298–2128
Zr (BCC)	−30706.0	264.284	−42.144	0	0	0	0	0	127.606	2128–4000
Zr (liquid)	10320.1	116.568	−24.162	−4.378	0	0.350	0	0.163	0	298–2128
Zr (liquid)	−8281.3	253.813	−42.144	0	0	0	0	0	0	2128–4000
Cu_5Zr	−108473.9	778.075	−144.73	−17.666	0.646	2.974	0	0	0	298–1271
$Cu_{51}Zr_{14}$	−1349480.0	8411.220	−1568.02	−196.790	6.590	31.660	0	0	0	298–1363
Cu_8Zr_3	−233709.6	1420.829	−265.39	−34.389	1.034	5.247	0	0	0	298–1176
$Cu_{10}Zr_7$	−374247.8	2184.396	−410.26	−57.214	1.292	7.696	0	0	0	298–1154
CuZr	−35702.3	248.502	−48.28	−7.035	0.129	0.525	0	0	0	298–1182
$CuZr_2$	−49290.0	372.136	−72.44	−11.413	0.129	1.224	0	0	0	298–1265

$G^\circ = a + bT + cT\ln(T) + dT^2 + eT^3 + f\backslash T + gT^4 + hT^7 + iT^{-9}$.

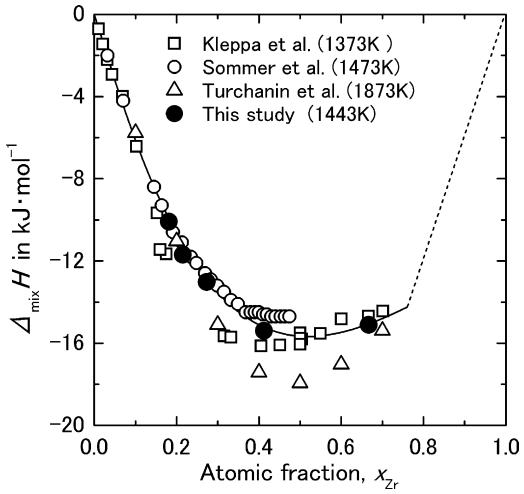

Fig. 7. Enthalpies of liquid–liquid mixing for the Cu–Zr alloys at 1443 K. (□) Kleppa and Watanabe (1373 K) [4], (◯) Sommer and Choi (1473 K) [5], (△) Turchanin and Nikolaenko (1873 K) [6], (●) This study (1443 K).

where $H_{1443} - H_{298}$ is the heat content of the Cu_mZr_n compound obtained in the present work, C_P the heat capacity of the pure copper or zirconium and $\Delta H_{m,Cu}$ is the enthalpy of fusion for the pure copper [12]. The $\Delta_f H^\circ_{298.15}$ values obtained and the literature values are listed in Table 5. $\Delta_f H^\circ_{298.15}$ of $CuZr_2$ agrees well with the values of Kleppa et al. [4] and Ansara et al. [8]. However, the values of Cu_9Zr_{12}, $Cu_{51}Zr_{14}$, Cu_8Zr_3 and $Cu_{10}Zr_7$ obtained in this study are in disagreement with previous reports [4,5,8], which may be due to the difference in the measured heat contents of the compounds.

The Gibbs energy values of the pure components of Cu and Zr, as well as those of the intermetallic compounds, and the ΔG^E coefficients for the liquid solution phase are summarized in Tables 6 and 7, respectively. Zeng et al. [14] and Arroyave et al. [15] carried out a similar thermodynamic optimization for this system, and their evaluated coefficients are in satisfactory agreement with the present ones. The phase diagram calculated with this set of evaluated coefficients is shown in Fig. 8, compared with that of Fig. 4 which was experimentally determined in the present study. It is found that both are in fairly good agreement. Fig. 9 shows the comparison between the assessed enthalpy, entropy and Gibbs energy of mixing of the liquid Cu–Zr system and the experimental data of enthalpy of mixing, respectively. The assessed values are about 2 kJ mol^{-1} higher than the experimental values. The activities of copper and zirconium (standard states: pure liquid copper and zirconium) at 1499 K were also calculated. They are shown in Fig. 10 against the mole fraction of

Table 7
Coefficients for the excess Gibbs energy of the liquid solution phase in the Cu–Zr system

ν	$A^{(\nu)}$ (J mol^{-1})	$B^{(\nu)}$ (J mol^{-1} K^{-1})
0	−59880	8.940
1	2987	−3.391
2	6303	−9.401

$L^{(\nu)}_{CuZr} = A^{(\nu)}_{CuZr} - B^{(\nu)}_{CuZr}T$.

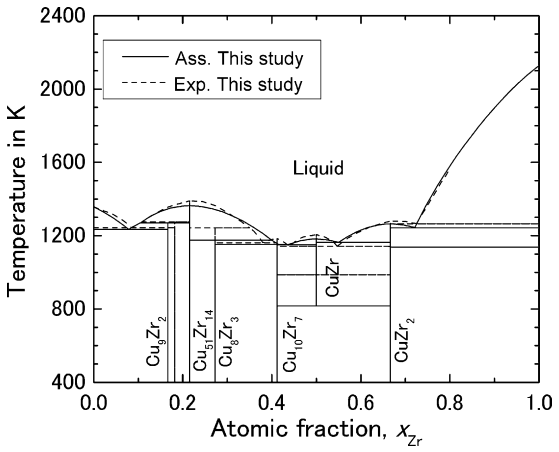

Fig. 8. Evaluated phase diagram of the Cu–Zr system: (—) assessed, (- - -) experimental.

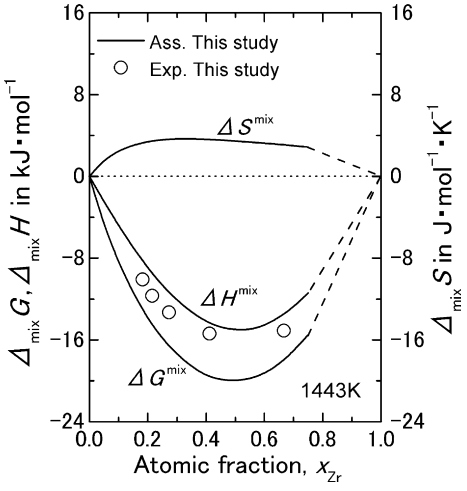

Fig. 9. Measured and evaluated thermodynamic properties of the Cu–Zr system at 1443 K: (—) assessed, (- - -) experimental.

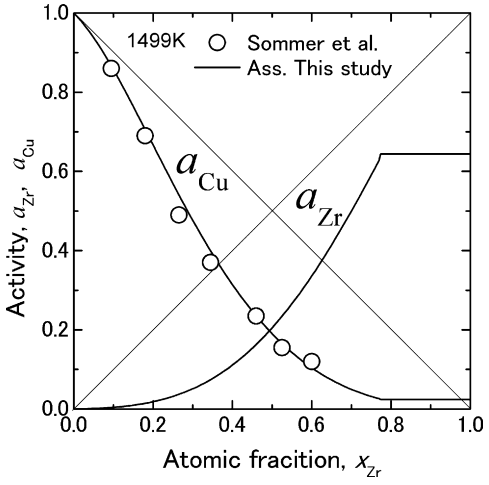

Fig. 10. Measured and evaluated activities of the Cu–Zr system at 1499 K (standard state: pure liquid Cu and Zr): (◯) Sommer and Choi [5], (—) assessed.

zirconium in comparison with those experimentally determined by Sommer and Choi [5]. It is also found that both agree fairly well.

5. Summary

The standard enthalpies of formation at 298.15 K for Cu_9Zr_2, $Cu_{51}Zr_{14}$, Cu_8Zr_3, $Cu_{10}Zr_7$ and $CuZr_2$ compounds are −23.8, −25.2, −16.2, −22.9 and −16.6 kJ g atom^{-1}, respectively. The phase relations and thermodynamic parameters in the Cu–Zr system were evaluated from the experimental information available in the literature. A set of optimized thermodynamic parameters has been derived to describe the Gibbs energies of the intermetallic compounds and that of the liquid phase. The calculated diagram as well as the invariant equilbria agree well with the experimental data.

References

[1] T.B. Massalski, Binary Alloy Phase Diagram, ASM, Ohio, 1990, p. 982.
[2] K. Itagaki, K. Matsuda, Japanese Patent, Application Number H9-219519 (1997).
[3] E. Kneller, Y. Khan, U. Gorres, Z. Metallkd. 77 (1986) 152.
[4] O.J. Kleppa, S. Watanabe, Met. Trans. B 13B (1982) 391–401.
[5] F. Sommer, D.K. Choi, Z. Metallkd. 80 (1989) 263–269.
[6] M.A. Turchanin, I.V. Nikolaenko, J. Alloys Compd. 236 (1996) 236–242.
[7] A.I. Zaitev, N.E. Zaitseva, Yu.P. Alekseeva, E.M. Kuril'chenko, S.F. Dunaev, Inorg. Mater. USSR 36 (2003) 816–825.
[8] I. Ansara, A. Pasturel, K.H.J. Buschow, Phys. Stat. Sol. (a) 69 (1982) 447–453.
[9] O. Redlich, A.T. Kister, Ind. Eng. Chem. 40 (1948) 345.
[10] K. Yamaguchi, K. Itagaki, J. Therm. Anal. Calori. 69 (2002) 1059–1066.
[11] K. Yamaguchi, Netsu Sokutei 31 (2004) 100–107.
[12] O. Knacke, O. Kubaschewski, K. Hesselmann, Thermochemical Properties of Inorganic Substances, Springer-Verlag, Berlin, 1991, p. 2370.
[13] G. Eriksson, K. Hack, Met. Trans. B 21B (1990) 1013–1023.
[14] K.J. Zeng, M. Hämäläinen, H.L. Lukas, J. Phase Equilib. 15 (1994) 577–586.
[15] R. Arroyava, T.W. Eager, L. Kaufman, J. Alloys Compd. 351 (2003) 158–170.